International Journal of Chemical, Materials and Biomolecular Sciences
ISSN: 2415-6620
Vol:8, No:5, 2014

The Strength and Metallography of a Bimetallic Friction Stir Bonded Joint between AA6061 and High Hardness Steel

Richard E. Miller

***Abstract*—**12.7-mm thick plates of 6061-T6511 aluminum alloy and high hardness steel (528 HV) were successfully joined by a friction stir bonding process using a tungsten-rhenium stir tool. Process parameter variation experiments, which included tool design geometry, plunge and traverse rates, tool offset, spindle tilt, and rotation speed, were conducted to develop a parameter set which yielded a defect free joint. Laboratory tensile tests exhibited yield stresses which exceed the strengths of comparable AA6061-to-AA6061 fusion and friction stir weld joints. Scanning electron microscopy and energy dispersive X-ray spectroscopy analysis also show atomic diffusion at the material interface region.

***Keywords*—**Dissimilar materials, friction stir, welding.

I. Introduction

SIMPLY described the friction stir welding (FSW) process involves a rotating machine tool, which is slowly plunged into the surface of a material construction joint (Fig. 1). Frictional heat is generated at the tool-to-material interface which softens the material to a state of plasticity and allows it to be deformed by the rotating tool action. After the local volume of joint material is fully heated, the rotating tool is then traversed along the joint face which stirs the adjoining material pieces to form a solid joint.

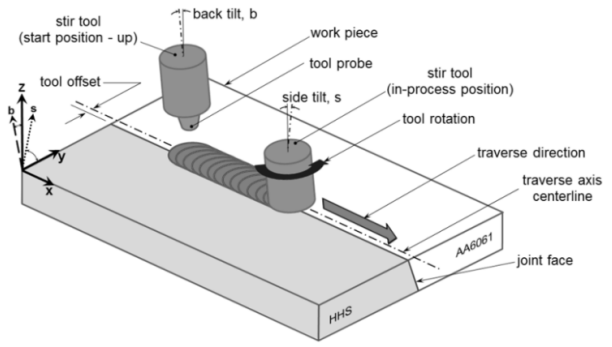

Fig. 1Schematic of friction stir process and terminology

Stemming from its initial application of joining aluminum alloys for the aerospace industry, the FSW process has been regularly used for joining metal components of like and dissimilar soft alloys; aluminum, magnesium, copper, etc. [1]. As tool design and construction has improved, FSW has been used for joining similar hard, high strength alloys such as steel and titanium [2] and has recently been applied to the joining of dissimilar metals i.e. aluminum and steel alloys [3].

As its name suggests FSW is a manufacturing method used to weld two materials together. A fundamental component of a welding process is heat. Fusion metal welding equipment delivers a high power heat source by electrical arc, laser, or electron beam to the weld area which then melts the immediate surfaces of the two adjoining pieces after which the molten area re-solidifies to create a single piece. For the friction stir process, the heat is provided not by electrical arc but primarily by the friction of the rotating tool as it rubs against the surfaces of the pieces to be joined. However unlike traditional welding, the materials are not melted but only softened to a state of plasticity. Because of its relatively low temperatures, FSW is a solid-state process that avoids the detrimental metallurgical effects associated with the liquid state welding processes.

Metals having chemical composition differences yield detrimental intermetallic compounds when melted and differing mechanical properties cause grain boundary or interstitial solution cracking which both make arc welding of dissimilar metals difficult. Microstructural transformations which occur as a metal is heated from solid to liquid state further compromise joint integrity by significantly decreasing material strength. However FSW has exhibited the ability to reduce or eliminate weld joint degradation and the detrimental effects of dissimilar material characteristics.

II. Materials and Methods

A coupon fixture mounted to a multi-axes friction stir welder (Transformation Technologies, Inc. GG1 Series) was used to join 12.7-mm thick x 25.4-mm wide x 200-mm long bars of AA6061-T6511 aluminum alloy and high hardness steel (HHS), Tables I and II respectively. Fig. 2 shows a completed bimetallic coupon. The FSW tool selected for this study was fabricated from a tungsten-rhenium alloy and featured a tapered probe. The sides of the material bars at the interface joint were machined to match the probe taper angle.

TABLE I
Chemical Composition of AA6061

	%Wt.		%Wt.		%Wt.
Al	Bal.	Cu	0.15-0.40	Cr	0.04-0.35
Si	0.40-0.80	Mn	0.15	Zn	0.25
Fe	0.7	Mg	0.8-1.2	Ti	0.15

R.E. Miller is with the Center for Advanced Technology at Focus: HOPE, Detroit, MI 48238 USA (phone 313-494-4716, e-mail: richard.miller@focushope.edu).

TABLE II
CHEMICAL COMPOSITION OF HIGH HARDNESS STEEL (528 HV)

	%Wt.		%Wt.		%Wt.		%Wt.
Fe	Bal.	Mo	0.21	Ni	0.4	S	0.003
C	0.28	Ti	0.045	V	0.01	Cr	0.5
Mn	0.87	Si	0.45	Al	0.041	Cu	0.05
P	0.011						

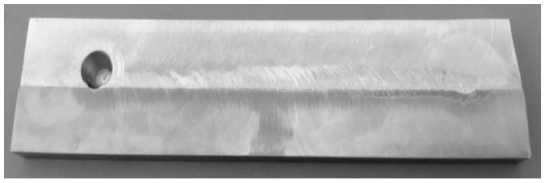

Fig. 2 Bimetallic FSW Coupon (top face milled)

Using positional control of the tool travel and visual inspection to assess weld quality, a series of process parameter trials was conducted to establish the operating limits of tool rotation speed, traverse speed, back tilt, and pre-traverse dwell time. Table III lists the parameter ranges applied during these trials.

TABLE III
FSW PROCESS PARAMETER RANGES

Plunge/Dwell	**Range**
Plunge tool rotation speed (RPM)	1000
Plunge rate (mm/min)	6 - 30
Dwell tool rotation speed (RPM)	300 - 600
Dwell duration (min)	2 - 3
Traverse	
Tool rotation speed (RPM)	250 - 500
Traverse rate (mm/min)	8 - 50
FSW Tool	
Pin diameter (in)	0.3 - 0.5
Pin pitch (degrees)	10.5 - 12
Spindle back tilt axis (degrees)	2 - 3
Spindle side tilt axis (degrees)	0 - 0.75
Rotation direction	CW/CCW
Bimetallic offset (mm)	0 - 2.5

Initial parameter sets expectedly produced unacceptable weld quality with excessive surface flash and considerable internal defects. After a series of parameter variations, the weld flash was reduced and externally-visible weld voids were eliminated. During a second series of parameter trials, saw-cut joint cross sections were used to determine internal weld quality for each parameter set and further parameters adjustments were made to eliminate weld voids and improve visual weld quality.

Finally based on the determined operating limits of tool rotation speed, traverse speed, and tool tilt angles, a series of coupons was fabricated using an experimental array methodology. Several tensile test specimens were extracted from each weld and then tested using an Instron Model 5982 testing machine. Mean tests results for each final series parameter set are shown in Table IV. Parameter Set #9 yielded the highest tensile strength of 204.5 MPa.

After determining the optimized process parameter set for tensile strength, additional coupons were fabricated using those parameters and test specimens were extracted by precision machining. Because AA6061 is a heat-treatable alloy and the FSW process temperatures were sufficient to alter the original temper of the base material (T6511) through annealing, approximately one-half of the bimetallic test specimens were subjected to aluminum alloy heat treatment.

TABLE IV
MEAN TENSILE STRENGTH OF PARAMETER OPTIMIZATION SPECIMENS

	Tool Rotation Speed (rpm)	Traverse Speed (mm/min)	Joint Offset (mm)	Back Tilt (°)	Side Tilt (°)	Sample Qty.	Mean Tensile Strength (MPa)
1	200	30	1.0	3.0	0.21	5	164.7
2	200	40	1.0	2.5	0.00	6	169.4
3	250	20	1.0	2.5	0.21	6	130.4
4	250	20	1.0	3.0	0.00	3	146.1
5	250	30	1.0	2.0	0.00	4	185.4
6	250	30	1.0	3.0	0.00	3	138.8
7	250	40	1.0	2.0	0.32	2	154.8
8	250	40	1.0	2.5	0.32	4	136.6
9	250	40	1.0	3.0	0.21	5	204.5
10	250	40	1.0	3.0	0.00	4	148.4
11	300	20	1.0	3.0	0.21	6	153.4
12	300	30	1.0	2.5	0.00	6	142.9
13	300	40	1.0	2.0	0.21	5	156.3
14	350	40	1.0	3.0	0.00	5	138.4

Because of the large disparity in the solidus temperatures of AA6061 and HHS, 582°C and 1400°C respectively, the bimetallic specimens were not subjected to steel heat treatment, which would have severely degraded the aluminum alloy. The full T6511 heat treatment process includes solution treating for one hour at 530°C followed by artificial aging (precipitation hardening) for eight hours at 175°C [4]. One-half of the heat-treated specimens received the full process and the remaining half was subjected to the precipitation/aging stage only.

III. RESULTS AND DISCUSSION

A. Mechanical Strength Testing

In addition to the tensile tests conducted during the parameter optimization phase, bending and shear strength of the as-welded, full heat treatment, and precipitation hardened specimens were was also conducted. [5], [6] Two types of bend specimens were extracted from the weld coupons to provide three test configurations of the force axis relative to the joint axis as shown in Fig. 3.

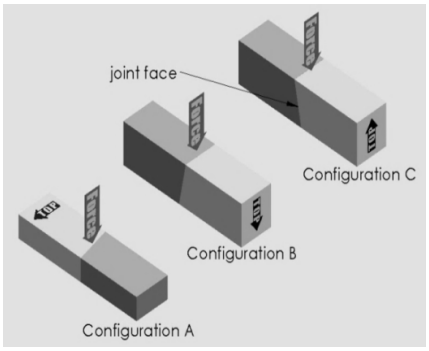

Fig. 3 Bend Test Force Configurations

Table V summarizes the results of the bending strength tests which indicated that the specimens that had been subjected to the full heat treatment process were significantly weaker than the as-welded and precipitation hardened samples. The bend test results indicate that the as-welded and precipitation-hardened specimens had nearly equivalent strength for all three force axis configurations. However the three configurations exhibited significantly different bending strength. Configuration B result was twice that of Configuration C and nearly seven times greater than Configuration A. With the lower side of the bend test specimens experiencing tension loading, this indicates that the joint tensile strength is stronger near the top face of the weld. This can be attributed to the upper portion of the weld joint receiving more frictional heat because of tool shoulder contact with the material's top face and/or the lower portion having less heat input because of the fixture plate contacting the material's bottom face and drawing heat out of the local material.

TABLE V
BENDING TEST RESULTS

	Mean Bend Strength (kN)		
Heat Treatment	**Bend A**	**Bend B**	**Bend C**
T6511	0.21	2.63	- - -
precipitation only	2.72	11.28	5.11
as-welded	2.72	10.34	5.92

TABLE VI
SHEAR TEST RESULTS

Heat Treatment	**Mean Shear Strength (MPa)**
precipitation only	163.2
as-welded	146.5

Table VI summarizes the results of the shear testing. Because the strength of the fully heat-treated bending test specimens was relatively low, shear test specimens were only subjected to precipitation-hardening. The test results indicate that the shear strength of the as-welded specimens were 10% weaker than the precipitation-hardened specimens.

B. Micro-Hardness Analysis

The friction stir process is known to significantly affect the hardness of the weld joint material. The primary causal factors for this phenomenon are the inherent process heat and work-hardening inflicted by the stirring plastic deformation of the stir tool. For the a heat-treatable aluminum alloy the hardest area of the FSW joint is the stir zone which is the result of grain refinement by dynamic recrystallization of the severely-deformed aluminum above the recrystallization temperature. In steel alloys the friction stir process typically increases material hardness and lowers hardness for aluminum alloys.

The hardness measurements were conducted using a LECO MAH43 automatic micro-hardness tester using a 500 gm load on steel and 100 gm load on aluminum because of the disparity in base material hardness. To facilitate the different loads between the two materials, two specimen mounts were created using transverse cross-section samples extracted adjacently from a weld coupon. Measurements were conducted at 1863 points (81 × 23 grid) on a 40-mm × 11-mm transverse cross-section of the bimetallic joint. The spacing between test points was 0.5-mm. Note that the hardness of the base materials was 110 HV for AA6061-T6511 plate and 550 HV for the HHS.

Fig. 4 is a micro-hardness profile of a transverse cross-section of the bimetallic AA6061-HHS FSW joint that was created by superimposing the micro-hardness profile of the steel (with its own scale) onto the aluminum alloy profile (also having its own scale).

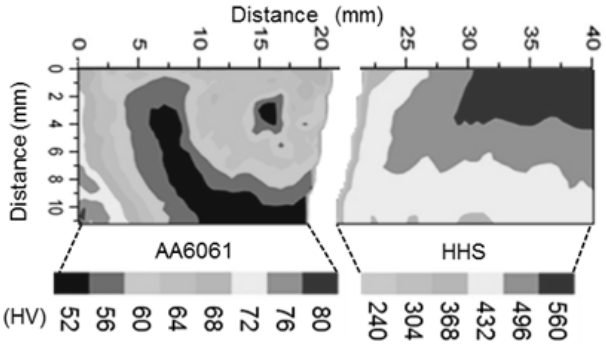

Fig. 4 Micro-hardness Profile of Bimetallic FSW Joint

The hardness of the steel is shown to vary from 240 HV at the joint interface to 560 HV in the top region away from the joint interface. The hardness levels generally decrease from top to bottom and right to the joint face (left). The micro-hardness profile of the aluminum exhibits a pattern typical of heat-treatable aluminum alloys by having a distinctly reduced hardness region corresponding to the thermo-mechanically-affected zone (TMAZ) of the weld joint. The aluminum hardness levels are the lowest, 52-56 HV, in the TMAZ and are 60-68 HV in the stir zone, or nugget. The central area of the stir zone also includes small veins of softer alloy, 52-56 HV. The hardest region of the aluminum material was 76-80 HV at the bottom surface of the work piece away from the joint interface.The inverse symmetry for the highest hardness regions of the aluminum and steel is most likely due to different heat transfer rates for each contact surface of the weld fixture.

C. Microstructure Analysis

Fig. 5 shows the microstructure of both the steel and aluminum sides of the joint cross-section with respect to the various micro-hardness regions exhibited in Fig. 4. The micro-hardness map indicates that the hardness of the steel is lowest at the bottom of the steel side near the bimetallic interface. The bottom region of the micro-hardness profile exhibits tempered martensitic microstructure with a hardness of 368-432 HV. The middle portion of the steel also shows tempered martensitic structure with a hardness of 432-496 HV. On the other hand, the top corner of the steel away from the joint interface exhibits martensitic microstructure and the highest hardness (496-560 HV) which is near the hardness level of the as-received steel plate. From the micro-hardness profile and microstructural morphology, we conclude that the lower portion of the steel substrate near the bimetallic joint interface slowly cooled after the stir tool had traversed through this area. As a result, well-tempered martensitic microstructure developed. On the other hand, the top-right corner of the sample was only marginally-affected by the frictional heat of the friction stir process because of its greater distance from the joint interface. As a result, the tempering effect was gradually reduced as the distance from the joint increased and consequently the material hardness gradually increased to a level near that of the as-received steel plate.

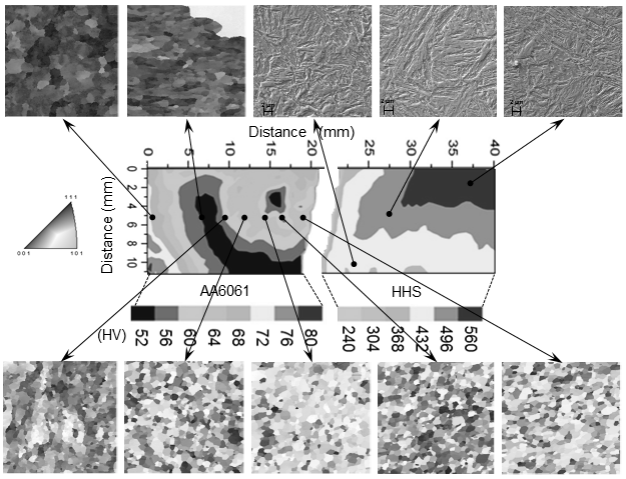

Fig. 5 Microstructure of Bimetallic FSW Joint

The microstructural morphology of aluminum at different positions of the weld was investigated using electron back scatter diffraction (EBSD) maps as shown in the upper left and bottom of Fig. 5. The EBSD investigation revealed that the grain size of the stir zone was reduced to about 5-10µm. Note that the grain size of the as-received AA6061-T6511 plate was about 100-500µm. During FSW, the material in the stir zone experienced large plastic deformation at high temperature. Consequently, the severely deformed material in the stir zone dynamically recrystallized to the smaller grain. The microstructure of the heat-affected zone (HAZ) shows the existence of sub-grains within the large grains. The color contrast of these grains suggests that the orientation of the sub-grains remain close to the parent grain. The sub-grains were probably developed by poligonization during thermal excursion due to the frictional heat generated during FSW.

D. Elemental Composition

An energy dispersive spectroscopy (EDS) investigation was done to evaluate the elemental distribution at the bimetallic joint interface. Fig. 6 shows the composition at three locations along the aluminum-steel joint interface. At the bottom and middle sections of the joint, the analysis revealed that a 1-2 µm thick intermetallic layer of Al and Fe had been atomically diffused at the joint interface. However at the top of the joint where the frictional heat input is highest, the layer was relatively thicker compared to the lower sections with thickness ranging 4-10µm. This is due to the relatively large heat generated at the top surface of the weld because of the frictional heat generated at the substrate/tool shoulder interface.

IV. Conclusions

This analysis indicates metallurgical bonding between the AA6061 aluminum and HHS alloys has occurred with an atomic diffusion zone 1-10µm wide at the bimetallic interface. Relative to the unwelded constituent materials the transverse tensile strength of the bimetallic FSW joint is significantly weaker, approximately half of the weakest unwelded base material AA6061. However relative to the comparative weld joint strengths of all-aluminum fusion and FSW weld joints, the tensile strength of the bimetallic friction stir weld is 65% stronger than that of a fusion-welded AA6061 joint and 5% stronger than a friction stir-welded AA6061 joint. Joint specimens that had been subjected to solution and/or precipitation hardening heat treatment were also subjected to bend and shear testing. These results indicate that the bending strength of bimetallic joints that had been both solution and precipitation hardened was inferior to that of joints that had only received precipitation treatment. Furthermore the results indicate that there is minimal strength difference between the as-welded and precipitation treated joint samples.

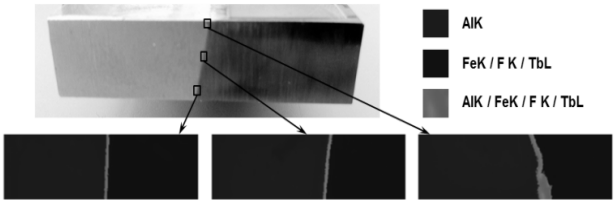

Fig. 6 Elemental Composition of Bimetallic FSW Joint

These positive results show that relatively soft AA6061 having a relatively low solidus temperature, and HHS having a high solidus temperature can be joined using the friction stir method. While the process developed here exhibited minimal stirring, or mechanical diffusion, between the two alloys because of the low tool offset angle, the metallurgical bonding

resulting from this method can be best described as friction stir bonding (FSB) which resulted from the proper temperature and forces being created by the stir tool at the bimetallic joint interface. By combining the attributes of low mass of the aluminum and strength, hardness, and durability of the high hardness steel,FSB provides a feasible construction technique for the merging of these disparate alloys.

ACKNOWLEDGMENT

This study was funded by the U.S. Army Tank and Automotive Research & Development Center.Dr. Guru P. Dinda, Associate Professor, Wayne State University, Detroit, MI provided metallurgical analysis and perspective.

REFERENCES

[1] W. M. Thomas, E. D. Nicholas., "Friction Stir Welding for the Transportation Industries", *Materials & Design, V.18, Iss. 4-6*, 1997 pp. 269-273.
[2] M. J. Gonser, "Microstructure Evolution and Material Flow Behavior in Friction-Stir Welded Dissimilar Titanium Alloys", (Doctoral dissertation), The Ohio State University, Columbus, OH, USA, 2010, retrieved from https://etd.ohiolink.edu/.
[3] R. E. Miller, "Preliminary Report on the Strength and Metallography of a Bimetallic Friction Stir Weld Joint Between AA6061 and MIL-DTL-46100E High Hardness Steel Armor", NTIS Technical Report #ADA580292, 2012, retrieved from http://www.ntis.gov.
[4] ASTM B918/B918M-9: Standard Practice for Heat Treatment of Wrought Aluminum Alloys, ASTM International
[5] ASTM D1002-10:Standard Test Method for Apparent Shear Strength of Single-Lap-Joint Adhesively Bonded Metal Specimens by Tension Loading (Metal-to-Metal), ASTM International
[6] ASTM E-290-13: Standard Test Methods for Bend Testing of Material for Ductility, ASTM International.